A Controllable Membrane-Type Humidifier for Fuel Cell Applications—Part I: Operation, Modeling and Experimental Validation

Denise A. McKay[1]
Picker Engineering Program,
Smith College,
Ford Hall, 100 Green Street,
Northampton, MA 01063
e-mail: dmckay@smith.edu

Anna G. Stefanopoulou
Fellow ASME
Mechanical Engineering,
University of Michigan,
1231 Beal Ave.,
Ann Arbor, MI 48109

Jeffrey Cook
Electrical Engineering,
University of Michigan,
1301 Beal Ave.,
Ann Arbor, MI 48109

For temperature and humidity control of proton exchange membrane fuel cell (PEMFC) reactants, a membrane based external humidification system was designed and constructed. Here we develop and validate a physics based, low-order, control-oriented model of the external humidification system dynamics based on first principles. This model structure enables the application of feedback control for thermal and humidity management of the fuel cell reactants. The humidification strategy posed here deviates from standard internal humidifiers that are relatively compact and cheap but prohibit active humidity regulation and couple reactant humidity requirements to the PEMFC cooling demands. Additionally, in developing our model, we reduced the number of sensors required for feedback control by employing a dynamic physics based estimation of the air-vapor mixture relative humidity leaving the humidification system (supplied to the PEMFC) using temperature and pressure measurements. A simple and reproducible methodology is then employed for parameterizing the humidification system model using experimental data. [DOI: 10.1115/1.4000997]

1 Introduction

A polymer electrolyte membrane fuel cell (PEMFC) chemically combines hydrogen and oxygen reactants to produce electricity, water, and heat. Because the PEMFC operates at low temperature sufficient for fast startup [1], it is considered as a viable power generator for automotive applications. To maintain high membrane conductivity and durability, the supplied gases require humidification. However, any excess water within the PEMFC can condense and affect performance [2], requiring accurate and fast control of the gas humidity supplied to the PEMFC [3].

Several humidification strategies have been considered for fuel cell reactant pretreatment. Although bubblers and spargers [4,5] are relatively inexpensive, and steam or hot plate injections are precise and fast, these technologies are not suitable for automotive applications due to either their cost, sluggish response, or large weight and volume. Alternatively, compact devices have been constructed that employ membrane-type humidifiers [6,7]. A membrane humidifier, shown in Fig. 1, directs dry gas across one surface of a polymeric membrane and hot liquid water (or a gas saturated with water vapor) across the other surface. Water vapor and thermal energy are exchanged through the membrane, from the liquid water to the dry gas, to heat and humidify the gas prior to entering the PEMFC.

Typically, membrane humidifiers are internal to the fuel cell stack and direct coolant water, or humidified fuel cell exhaust gas, from the power producing portion of the PEMFC to the humidifier to heat and humidify the supplied gas [8–10]. These humidifiers are designed to fully humidify the gas at the temperature of the coolant exiting the PEMFC. While these internal humidifiers are relatively compact and simple with respect to control, they prohibit active humidity regulation and couple reactant humidity requirements to the PEMFC cooling demands. For example, during a tip-out (load reduction), the requested air mass flow rate decreases, resulting in an increase in relative humidity. When operating at high cathode supply humidities (typical of low to moderate current densities, this relative humidity increase will cause condensation and flooding, additionally resulting in the nonuniform distribution of reactants to the individual cells. Conversely, a tip-in results in membrane dehydration during fast transients. Regulation, and thus active control, during these transients is critical for optimal fuel cell performance. To overcome the humidity constraints of passive humidifiers, sliding plates were considered to activate and deactivate gas channels within the internal humidifier to control the contact area between the liquid and gas [11].

The humidification system considered here decouples the passive humidifier from the PEMFC cooling loop and employs a gas bypass for humidity control, conceptually similar to Ref. [12]. It is important to note here that it is not the conceptual system design that is novel, rather the control (which necessitates a model). To design adequate controllers for thermal regulation (using heaters) and humidity control (for the gas flow split between the humidifier and bypass), we developed a low-order, control-oriented model based on first principles. Similar to engine thermal management systems employing either a valve or servo motor to bypass coolant around the heat exchanger [13–15], the coordination of the heaters and the bypass valve is challenging during fast transients due to the different time scales, the actuator constraints, and the sensor responsiveness.

The additional complexity in this application arises from the need to avoid condensation of the water vapor carried by the humidified gas stream. The low-order control-oriented model developed here will enable systematic controller tuning of the multiple interconnected thermal loops, better sizing of the actuators (heaters), and sensor selection and placement. This model of the humidification system can be used to design and tune controllers for thermal and humidity regulation for reference tracking and disturbance rejection, as described in Part B of this work.

[1]Corresponding author.

Contributed by the Heat Transfer Division of ASME for publication in the JOURNAL OF FUEL CELL SCIENCE AND TECHNOLOGY. Manuscript received March 31, 2008; final manuscript received October 29, 2009; published online July 16, 2010. Review conducted by Ken Reifsnider.

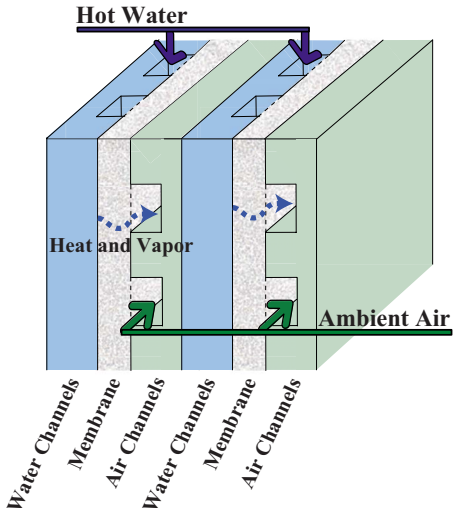

Fig. 1 Schematic diagram of a two-cell membrane based humidifier

First, a description of the membrane based gas humidification system and hardware is provided in Sec. 2. An estimate of the relative humidity of the gas supplied to the PEMFC (exhaust from the humidification system) is presented and experimentally validated in Sec. 3. Then, the physics based model of the humidification system is presented in Sec. 4 followed by the methodology used to identify the unknown parameters in Sec. 5. The model is experimentally validated in Sec. 6, followed by a discussion of the steady system efficiency at various operating conditions in Sec. 7.

2 Humidifier System and Hardware

The experimental hardware, designed in collaboration with the Schatz Energy Research Center at Humboldt State University, was installed in the Fuel Cell Control Laboratory at the University of Michigan. The system was designed to deliver moist air at 45–70°C and 50–100% relative humidity at dry air mass flow rates up to 40 slm, corresponding to 300% excess oxygen in the cathode of a 0.5 kW fuel cell. Although the humidifier gas delivery system can accommodate either the anode feed gas (hydrogen) or the cathode feed gas (air), this work focuses on the task of humidifying the air stream supplied to the PEMFC cathode.

A detailed schematic of the humidification system hardware is provided in Fig. 2, illustrating the location of the sensors and actuators used to control and monitor the gas humidification system. A standard desktop computer was equipped with data acquisition boards, along with a signal conditioning system, to control and monitor the humidification system.

The humidifier system consists of five control volumes, namely, the water heater, humidifier, water reservoir, air bypass, and gas mixer. Figure 3 shows the interaction of the air and liquid water as they move through these control volumes, where the letter *T* in

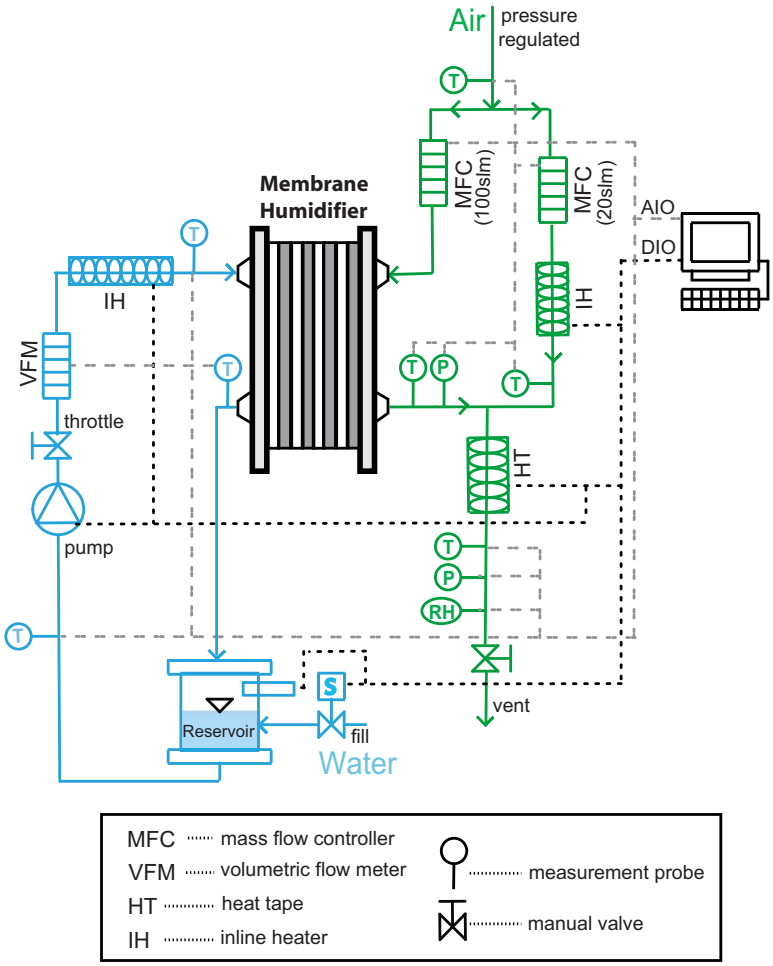

Fig. 2 Schematic of the gas humidification system, detailing sensor, and actuator hardware (with plumbing indicated in solid lines) along with the computer signal communication (with wiring indicated in dotted lines)

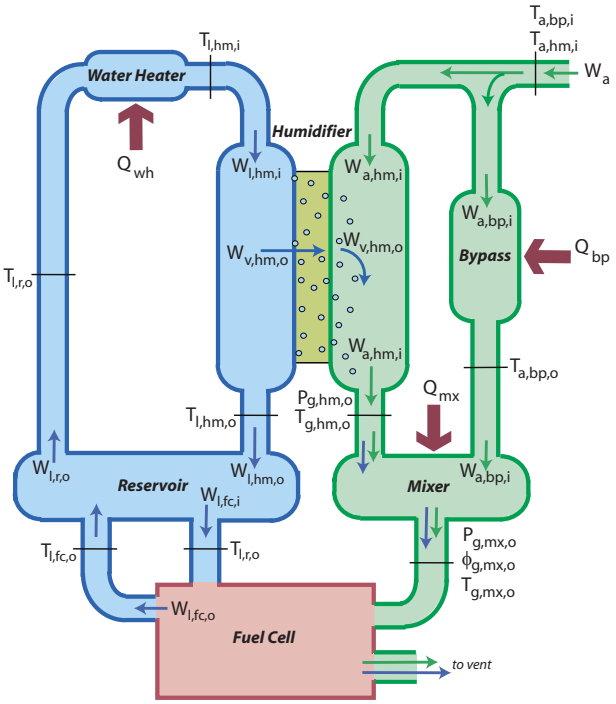

Fig. 3 Controllable humidifier system indicating states, disturbances, and measurements. Thin arrows represent mass flow directions and large thick arrows indicate locations where control action is applied.

(K) is used to denote temperature, P in (Pa) for pressure, W in (kg/s) for mass flow rate, Q in (W) for heat added to a control volume, and r for the fractional flow diverted through the bypass. Subscripts are used to indicate first the substance of interest, where a is for air, b is for bulk materials, g is for gas (often indicating a mixture such as air and water vapor), l is for liquid water, and v is for water vapor; second, the control volume such as bp is for bypass, cv is generically for control volume, r is for reservoir, fc is for fuel cell, wh is for water heater, hm is for humidifier, and mx is for mixer; finally, an i or o indicates the control volume inlet or outlet.

Two mass flow controlled streams of dry air are supplied to the bypass $W_{a,\mathrm{bp},i}$ and the humidifier $W_{a,\mathrm{hm},i}$. The number of cells in the humidifier and the membrane surface area were chosen to ensure that the humidifier produces a saturated air stream at a temperature $T_{g,\mathrm{hm},o}$ dependent upon the supplied liquid water temperature $T_{l,\mathrm{hm},i}$ for the range of humidifier air mass flow rates expected. The air bypassing the humidifier is heated, with a 50 W resistive heater Q_{bp} to the temperature of the air exiting the humidifier. This saturated air stream (from the humidifier) and dry air stream (from the bypass) are combined in the mixer to produce a desired air-vapor mixture relative humidity $\phi_{g,\mathrm{mx},o}$ to be supplied to the PEMFC. A 52 W resistive heater Q_{mx} is used in the mixer for temperature control and to minimize condensation during the mixing of the saturated and dry air streams.

When the humidifier system is coupled with a PEMFC, the total mass flow of dry air through the bypass and the humidifier W_a is a function of the current produced by the PEMFC stack as well as the desired stoichiometric ratio (fraction of the air flow rate in excess of that required to sustain the chemical reaction in the PEMFC). Thus, the dry air mass flow rate can be thought of as a disturbance to the humidifier system, while the fraction of the air that is supplied to the bypass r_{bp} or humidifier is controllable.

Liquid water stored in a reservoir is circulated through the water heater and humidifier before returning to the reservoir. The water circulation system contains a water pump, manual throttle valve, and water flow meter for controlling and monitoring the liquid water flow rate. The water reservoir is shared with the fuel cell coolant loop, containing a heat exchanger, fan, and circulation pump, which are not shown. Liquid water from the fuel cell is an input to the reservoir at the fuel cell coolant temperature $T_{l,\mathrm{fc},o}$. To mitigate thermal disturbances in the reservoir (such as reservoir fill events or temperature cycling in the PEMFC), increase the humidifier thermal response time, offset heat losses to the ambient, and provide the energy required to evaporate liquid water, a 1000 W resistive heater Q_{wh} is used to heat the liquid water before entering the humidifier. This heater will be referred to as the "water heater."

Table 1 Nominal system operating conditions

Variable	Nominal value
$W^o_{a,\mathrm{hm},i}$	0.42 g/s
$W^o_{a,\mathrm{bp},i}$	0.18 g/s
$T^o_{a,\mathrm{hm},i}=T^o_{a,\mathrm{bp},i}$	20°C
$W^o_{l,\mathrm{hm},i}$	30 g/s
T^o_{amb}	27°C
$p^o_{g,\mathrm{hm},o}$	102.57 kPa absolute
$T^o_{a,\mathrm{bp},o}=T^o_{g,\mathrm{hm},o}$	55°C

Nominal operating conditions were selected for control purposes, as described in Part B of this work, and are provided here for reference. These nominal conditions were selected to approximate the midpoint of the expected stack operating range while applying a 0.3 $\mathrm{A/cm^2}$ fuel cell electric load at a cathode air stoichiometry of 250%.

In order to evaporate liquid water on the liquid side of the membrane gas humidifier, to be exchanged through the membrane to the air, energy must be provided. This energy can be provided either directly through the water heater or indirectly by increasing the temperature of the coolant exhaust from the fuel cell stack, which is provided to the humidifier through the coupled water reservoir. This design choice influences the water heater sizing and influences the control objectives associated with temperature regulation, as described below and in more detail in the second part of this two-paper series. It is important to note that the model presented in this work treats the fuel cell coolant outlet temperature as an input to the water reservoir, which could be neglected if so desired.

In sizing the water heater, if the temperature of the gas supplied to the PEMFC tracked the temperature of the coolant leaving the PEMFC, and assuming no heat losses between the fuel cell, water reservoir, water heater, and the humidifier, then the water heater would provide the exact amount of energy needed to evaporate water (enthalpy of vaporization) under a specific set of operating conditions. Under the nominal conditions indicated in Table 1, the energy required to evaporate water is approximately 160 W. However, the water heater should be sized to provide all of the energy required to evaporate liquid water at the maximum operating temperature and gas flow rate $T_{g,\mathrm{hm},o}=70$°C, $W_{a,\mathrm{hm},o}=0.82$ g/s resulting in a requirement for at least 500 W. Additionally, sensible heat is transferred from the liquid water to the air due to the thermal gradient through the membrane, requiring approximately 35 W. Finally, the humidifier is not adiabatic (with no insulation) and thus the water heater must also be sized to account for heat loss to the ambient due to natural convection, which is expected to be approximately 200 W under these maximum operating conditions (greatest thermal gradient). The resulting maximum water heater power requirement is thus approximately 735 W to account for the enthalpy of evaporation, sensible heat, and heat loss to the ambient.

As a design note, if the liquid water were supplied to the water reservoir from the PEMFC at a temperature greater than that required of the gases supplied to the PEMFC, this energy input into

the water reservoir could be used to reduce the amount of heat provided by the water heater. Such a technique has an added benefit of reducing the amount of heat rejected by the heat exchanger in the PEMFC coolant loop. The system model presented in this paper accounts for the PEMFC coolant exhaust temperature injected into the water reservoir, both for purposes of examining this disturbance as well as for consideration in reducing the water heater energy requirement. The influence of this coolant temperature on steady system efficiency is examined in detail in Sec. 7.

The membrane based humidifier employs solid expanded Teflon (ePTFE) GORE® SELECT™ ionomer composite membranes for water vapor transport from the liquid water to the air. Air and liquid water are transported to opposite sides of the 300 cm^2 humidifier membranes using channels milled into sheets of polypropylene. The humidifier membranes also contain bonded sheets of polytetrafluoroethylene (PTFE) gaskets for sealing purposes. Finally, the channels and membranes are held together with phenolic endplates used to maintain cell compression.

To eliminate the need for a relative humidity probe, as discussed in detail in Sec. 3, the humidifier membrane surface area was carefully selected to ensure that the air-vapor mixture leaving the humidifier is always saturated for the range of air mass flow rates of interest. This design result has been confirmed experimentally under the range of expected system operating conditions. The temperature at which the air leaves the humidifier, thus, how much water the air holds when saturated, depends on the liquid water temperature on the liquid side of the humidifier membranes. This liquid water temperature, in turn, depends on the water heater input. As a result, under the expected range of operating conditions, the air-vapor mixture will always be saturated at the humidifier outlet at a temperature that depends on the water heater input.

Finally, the water reservoir must be sized appropriately to ensure that the water supply is not depleted by humidifying the air. If reservoir sizing were of interest, one could recapture the water in the saturated fuel cell exhaust streams to significantly reduce the frequency with which the water reservoir must be filled. However, full water recovery cannot be realistically achieved resulting in occasional reservoir filling as would be the case for an internally humidified fuel cell stack.

3 Relative Humidity Estimation

The relative humidity of the air supplied to the PEMFC from the mixer, considered as a system output, must be known to ensure adequate controller performance. To reduce the number of sensors used for feedback control, a methodology was established for estimating the humidity of the air leaving the mixer to be supplied to the fuel cell cathode. This approach avoids having to rely on two sensors (humidity and temperature) and works well for compensating for the slow humidity sensor response at saturation due to condensation during operation at high humidity conditions. This estimation will be compared with a relative humidity measurement with an accuracy of 1.5% using a Rotronic SP05 capacitive relative humidity probe.

The water vapor mass flow rate of a gas-vapor mixture of varying composition cannot be directly measured and must instead be estimated based on variables that can be measured, namely temperature, total pressure, and dry air mass flow rate. Applying the definition for the humidity ratio $\omega = M_v \phi P^{\text{sat}} / M_a (P - \phi P^{\text{sat}})$, the water vapor mass flow rate exiting a control volume is described by

$$W_{v,\text{cv},o} = \frac{M_v \phi_{g,\text{cv},o} P^{\text{sat}}_{g,\text{cv},o}}{M_a (P_{g,\text{cv},o} - \phi_{g,\text{cv},o} P^{\text{sat}}_{g,\text{cv},o})} W_{a,\text{cv},o} \quad (1)$$

where M_a is the molar mass of air (kg/mol) and M_v is the molar mass of water (kg/mol). For reference, at nominal operating conditions, the water vapor mass flow rate leaving the humidifier is approximately $W_{v,\text{hm},o} = 0.068$ g/s at a dry air mass flow rate through the humidifier of $W_{a,\text{hm},o} = 0.42$ g/s.

To estimate the relative humidity in the mixer outlet, mass conservation is applied to both the air and water vapor. First, the mass flow rate of water vapor leaving the humidifier is assumed equal to that leaving the mixer $W_{v,\text{hm},o} = W_{v,\text{mx},o}$. Then, the air mass flow rate entering the mixer from the humidifier $W_{a,\text{hm},i}$ and the bypass $W_{a,\text{bp},i}$ is assumed equal to that leaving the mixer $W_a = W_{a,\text{hm},i} + W_{a,\text{bp},i}$. By substituting the equation for the conservation of air mass into the equation for the conservation of water mass and applying the definition of the water vapor mass flow rate from Eq. (1), the relative humidity of the mixer outlet can be expressed by

$$\phi_{g,\text{mx},o} = \phi_{g,\text{hm},o} r_{\text{hm}} \frac{P^{\text{sat}}_{g,\text{hm},o}}{P^{\text{sat}}_{g,\text{mx},o}} \left(\frac{P_{g,\text{mx},o}}{P_{g,\text{hm},o} - r_{\text{bp}} \phi_{g,\text{hm},o} P^{\text{sat}}_{g,\text{hm},o}} \right) \quad (2)$$

where $\phi_{g,\text{hm},o}$ and $\phi_{g,\text{mx},o}$ are the relative humidities at the humidifier and mixer outlets, respectively; $P_{g,\text{hm},o}$ and $P_{g,\text{mx},o}$ are the humidifier and mixer outlet total pressures (Pa); $r_{\text{bp}} = W_{a,\text{bp},i} / W_a$ and $r_{\text{hm}} = W_{a,\text{hm},i} / W_a$ are the fractions of the total air mass flow through the bypass and humidifier, respectively; and $P^{\text{sat}}_{g,\text{hm},o}$ and $P^{\text{sat}}_{g,\text{mx},o}$ are the water vapor saturation pressures evaluated at the temperature of the air-vapor mixture leaving the humidifier $T_{g,\text{hm},o}$ and leaving the mixer $T_{g,\text{mx},o}$, respectively (Pa). The water vapor saturation pressure is a function of temperature by fitting data provided in standard thermodynamic steam-tables [16]. The humidifier and mixer gas outlet temperatures $T_{g,\text{hm},o}$ and $T_{g,\text{mx},o}$ enter the equation through this functional relationship of the saturation pressure on temperature.

By designing the membrane humidifier such that the air outlet is fully humidified $\phi_{g,\text{hm},o} = 1$, as described in Sec. 2, the reliance on a relative humidity sensor for feedback control can be eliminated. Should the humidifier not provide a saturated air-vapor mixture, then the relative humidity of this air-vapor mixture must be measured in order to employ Eq. (2). In such a case, the mixer outlet relative humidity should be directly measured, rather than employing Eq. (2), and reliance on a relative humidity measurement cannot be avoided.

This model of the mixer outlet relative humidity, in Eq. (2), is physics based, depends only on measured variables, and does not contain parameters requiring identification. The measurement inputs to the model are the dry air mass flow rates supplied to the humidifier and bypass and the gas temperatures and total pressures at the humidifier and mixer outlets. The estimated and measured mixer outlet relative humidities were compared under a range of operating conditions, shown in Fig. 4.

To examine the estimation error, the measured and estimated mixer outlet relative humidities are compared, as shown in Fig. 5. The average estimation error was found to be 3.8% relative humidity with a standard deviation of 1.6% relative humidity, approximately two times greater than the accuracy of the relative humidity sensor. This estimation error is not symmetric about the measured value. Instead, the estimation is, on average, consistently 3.8% relative humidity less than the measurement. Although not significant, this error is predominantly due to the nearly constant bias in the measurement. This bias is thought to result from the inaccessible temperature probe embedded in the relative humidity transducer being calibrated against a different temperature standard than that used to calibrate the mixer and humidifier outlet temperatures. Of critical importance, the relative humidity estimator accurately captures the dynamic response throughout the experiment.

Removing this bias in the measurement, by adding the 3.8% relative humidity bias to the estimation over the range of testing conditions, results in an improved estimation, as shown in Fig. 6 for the same experiment. The average estimation error for the bias corrected relative humidity estimation was then found to be 1.2% relative humidity with a standard deviation of 1.6%, which is less than the sensor accuracy.

These results have shown that with accurate measurements of temperature, the dynamic response of relative humidity can be

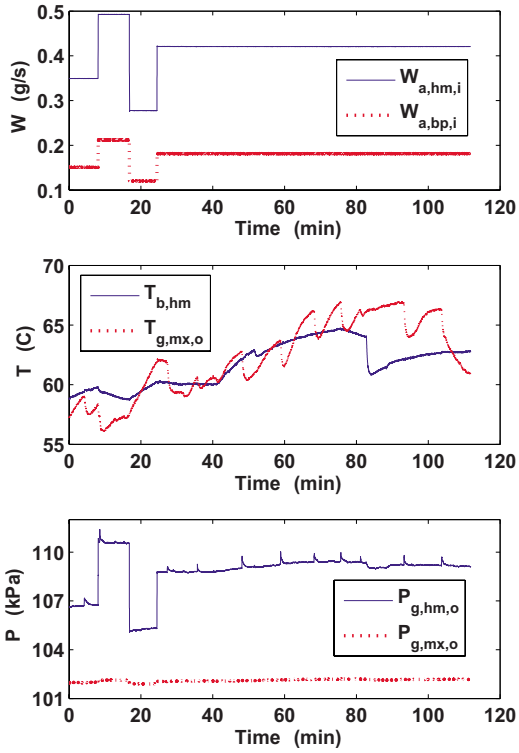

Fig. 4 Experimental inputs to the relative humidity estimator

adequately estimated under a range of operating conditions typical for this system. Moreover, they indicate that the gas relative humidity can be accurately controlled if the temperature can be well regulated. As a result, the thermal dynamics of the various control volumes, related time constants, and impact of the operating conditions on the thermal response must be well understood to generate an accurate estimation of gas temperatures. As a means to this end, a physics based, low-order model will be developed to estimate the system thermal dynamics.

4 System Modeling

Applying the conservation of mass and energy to each of the control volumes, as well as the properties of gas-vapor mixtures, expressions for the thermal dynamics were formulated resulting in an eight state system. The following general assumptions were made in developing the model due to the expected range of system operating temperatures (25–70°C), pressures (close to atmospheric), and resulting thermal gradients.

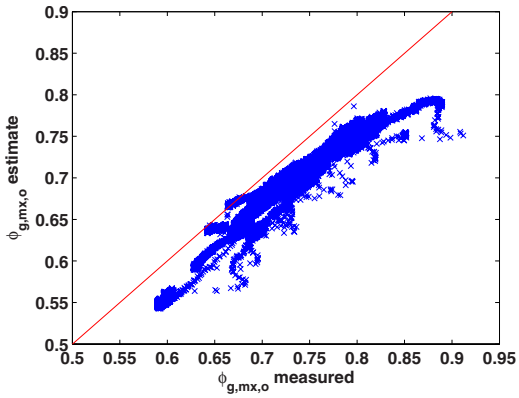

Fig. 5 Relative humidity estimator experimental validation

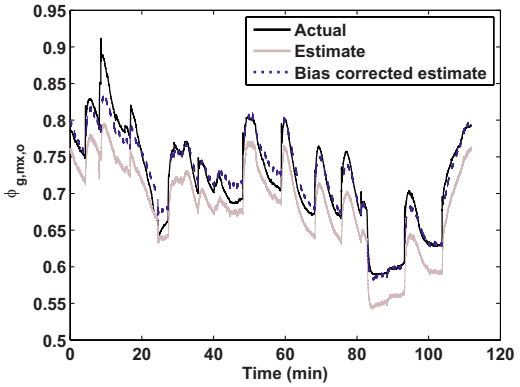

Fig. 6 Relative humidity estimation as compared with the measurement versus time after removing the estimation bias

- A1. There is no radiative heat loss from the control volumes. Heat loss to the surroundings is assumed to be a linear function of the difference in temperature as a result of natural convection alone. This assumption is made for model simplicity, to reduce the number of unknown parameters requiring experimental identification, and will result in an overestimation of the convective heat losses by effectively lumping both convection and radiation effects.
- A2. Under the range of operating temperatures and pressures considered, and assuming liquid water and air are incompressible, there is no change in mass stored within the control volumes. If the control volumes are significantly larger than considered in this work, or if the mass flow response is significantly slower causing a flow lag (as expected for an air compressor or blower), then this assumption should be revisited.
- A3. All constituents have constant specific heat and all gases behave ideally. Under the range of operating temperatures and pressures considered, this assumption is justified; however, extensions to higher temperature or pressure should be made with caution.
- A4. Each control volume is homogenous and lumped parameter. This assumption is made for simplicity since the model is intended for controller design. Caution should be used if extending this work to elucidate design implications.

Many of the control volumes within the humidification system have striking similarities. Therefore, a generalized two volume model will first be presented in Sec. 4.1. The membrane humidifier model will then be developed in Sec. 4.3. Following the presentation of the detailed system thermal model in Sec. 4.2, the heat transfer coefficients in Eq. (3) will be experimentally identified in Sec. 5.

4.1 General Two Volume Model. Each control volume is comprised of the material flowing through it, consisting of gases and/or liquid water and the bulk materials that contain it, such as stainless or acrylic. A general description of the heat transfer mechanisms and constituent flows are shown in Fig. 7 for a gas flowing through a control volume made up of bulk materials. Note, this same schematic is used to represent the volumes containing liquid water by simply changing the subscript from g to l. However, the humidifier control volume obviously has increased complexity due to the exchange of mass and energy across the polymeric membrane and will be described in more detail after the presentation of this simple case.

The temperature state $T_{b,\mathrm{cv}}$ represents the lumped temperature of the bulk materials, which make up the control volume and the gas temperature state $T_{g,\mathrm{cv}}$ represents the temperature of the gases inside the control volume (between the bulk materials). Gas is supplied to the control volume at a specified mass flow rate $W_{g,\mathrm{cv},i}$

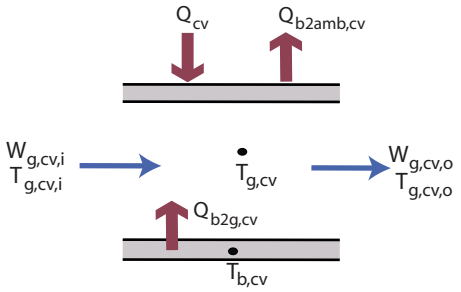

Fig. 7 General description of the heat transfer mechanisms for control volumes containing bulk and gas states

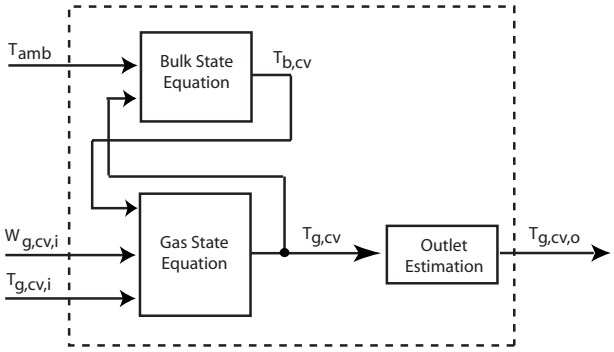

Fig. 8 Simulation schematic of the general two volume system

and temperature $T_{g,\mathrm{cv},i}$. Gas leaves the control volume at $W_{g,\mathrm{cv},o}=W_{g,\mathrm{cv},i}$, at the temperature $T_{g,\mathrm{cv},o}$. Heat is transferred to the bulk materials through a resistive heater, denoted by Q_{cv}, which then transfers by forced convection from the bulk materials to the gases by $Q_{b2g,\mathrm{cv}}=\hbar_{b2g,\mathrm{cv}}A_{b2g,\mathrm{cv}}(T_{b,\mathrm{cv}}-T_{g,\mathrm{cv}})$. Heat transfer from the bulk materials to the ambient occurs via natural convection and is represented by $Q_{b2\mathrm{amb},\mathrm{cv}}=\hbar_{b2\mathrm{amb},\mathrm{cv}}A_{b2\mathrm{amb},\mathrm{cv}}(T_{b,\mathrm{cv}}-T_{\mathrm{amb}})$. The heat transfer coefficients associated with forced convection are a function of the mass flow rate $\hbar_{b2g,\mathrm{cv}}=\beta_{b2g,\mathrm{cv},1}(W_{g,\mathrm{cv},i})^{\beta_{b2g,\mathrm{cv},2}}$, where as the heat transfer coefficients associated with natural convection are constant $\hbar_{b2\mathrm{amb},\mathrm{cv}}=\beta_{b2\mathrm{amb},\mathrm{cv}}$.

State equations are then expressed for the bulk and gas (or liquid water) states by applying the conservation of mass and energy, resulting in

$$\frac{dT_{g,\mathrm{cv}}}{dt}=\frac{1}{m_{g,\mathrm{cv}}C_{g,\mathrm{cv}}}[W_{g,\mathrm{cv},i}C_{p,g}(T_{g,\mathrm{cv},i}-T_{g,\mathrm{cv},o})+\hbar_{b2g,\mathrm{cv}}A_{b2g,\mathrm{cv}}(T_{b,\mathrm{cv}}-T_{g,\mathrm{cv}})] \tag{3a}$$

$$\frac{dT_{b,\mathrm{cv}}}{dt}=-\frac{1}{m_{b,\mathrm{cv}}C_{b,\mathrm{cv}}}[-\hbar_{b2g,\mathrm{cv}}A_{b2g,\mathrm{cv}}(T_{b,\mathrm{cv}}-T_{g,\mathrm{cv}})-\hbar_{b2\mathrm{amb},\mathrm{cv}}A_{b2\mathrm{amb},\mathrm{cv}}(T_{b,\mathrm{cv}}-T_{\mathrm{amb}})+Q_{\mathrm{cv}}] \tag{3b}$$

where the letter C is used to denote the constant volume specific heat of the control volume (J/kg K), C_p is the constant pressure specific heat of the control volume (J/kg K), m is the control volume mass (kg), and A is the surface area through which heat is transferred (m^2). Additionally, the subscript amb is used for ambient. When heat flows between two materials, the heat transfer coefficients and surface areas will use subscripts with the numeral 2 between the two substances of interest, for example, a heat transfer between the bulk materials and the ambient will be denoted by $b2$amb.

The internal gas temperature state is not directly measured. As a result, some approximation of the control volume temperature distribution must be made in order to compare the model estimates to measured values, either for model calibration or for control. It is therefore generally assumed that the gas temperature $T_{g,\mathrm{cv}}$ is a linear average between the inlet and outlet temperatures, such that

$$T_{g,\mathrm{cv},o}=2T_{g,\mathrm{cv}}-T_{g,\mathrm{cv},i} \tag{4}$$

It is important to keep in mind that the subsystem outlet temperatures are regulated, not the internal states, and thus a good approximation of these outlet conditions will guide the controller tuning and will be confirmed through model validation.

For the control volumes that contain bulk temperatures that are not directly measured (reservoir, water heater, and mixer), the states within these systems must remain coupled during simulation. This coupling implies that the state estimations serve as inputs to each other. For example, the estimation of the gas temperature state $T_{g,\mathrm{cv}}$ is an input to the model estimate of the bulk temperature $T_{b,\mathrm{cv}}$ and vice versa, as shown in Fig. 8. The outlet estimation of Eq. (4) is used for comparison with the measurement.

4.2 Detailed Model. Applying the general model framework from Sec. 4.1 to the humidification system results in an 11 state system, with two temperature states for the reservoir, water heater, bypass, and mixer, and three temperature states for the humidifier. Employing the parameter identification methodology, described in Sec. 5, and examining the system response, it was found that both the humidifier and the bypass models can be simplified. The identified heat transfer coefficient from the air to the bulk materials in the humidifier was found to be approximately zero, indicating that the predominant heat transfer is between the bulk and the liquid water and then from the bulk to the ambient. By lumping the humidifier bulk and liquid water into a single state, the humidifier control volume was reduced from three to two states while still adequately estimating the thermal dynamics. The bypass utilizes an inline heater with a heating element in intimate contact with the gas, as compared with the mixer that utilizes heat tape. Due to the very fast gas dynamics of dry air, the bypass can be reduced to a single state system and still capture the response time due to changes in both the air mass flow rate and heat supplied.

The resulting state equations are expressed for the bypass

$$\frac{dT_{\mathrm{bp}}}{dt}=\frac{1}{m_{\mathrm{bp}}C_{\mathrm{bp}}}[Q_{\mathrm{bp}}+W_{a,\mathrm{bp},i}C_{p,a}(T_{a,\mathrm{bp},i}-T_{a,\mathrm{bp},o})-\hbar_{\mathrm{bp}}A_{\mathrm{bp}}(T_{\mathrm{bp}}-T_{\mathrm{amb}})] \tag{5}$$

the water heater

$$\frac{dT_{l,\mathrm{wh}}}{dt}=\frac{1}{m_{l,\mathrm{wh}}C_{l,\mathrm{wh}}}[W_{l,\mathrm{hm},i}C_{p,l}(T_{l,r,o}-T_{l,\mathrm{hm},i})+\hbar_{b2l,\mathrm{wh}}A_{b2l,\mathrm{wh}}(T_{b,\mathrm{wh}}-T_{l,\mathrm{wh}})] \tag{6a}$$

$$\frac{dT_{b,\mathrm{wh}}}{dt}=\frac{1}{m_{b,\mathrm{wh}}C_{b,\mathrm{wh}}}[Q_{\mathrm{wh}}-\hbar_{b2l,\mathrm{wh}}A_{b2l,\mathrm{wh}}(T_{b,\mathrm{wh}}-T_{l,\mathrm{wh}})-\hbar_{b2\mathrm{amb},\mathrm{wh}}A_{\mathrm{wh}}(T_{b,\mathrm{wh}}-T_{\mathrm{amb}})] \tag{6b}$$

the water reservoir

$$\frac{dT_{l,r}}{dt}=\frac{1}{m_{l,r}C_{l,r}}[W_{l,\mathrm{fc},i}C_{p,l}(T_{l,\mathrm{fc},o}-T_{l,r,o})+W_{l,\mathrm{wh},i}C_{p,l}(T_{l,\mathrm{hm},o}-T_{l,r,o})-\hbar_{l2b,r}A_{l2b,r}(T_{l,r}-T_{b,r})] \tag{7a}$$

$$\frac{dT_{b,r}}{dt}=\frac{1}{m_{b,r}C_{b,r}}[\hbar_{l2b,r}A_{l2b,r}(T_{l,r}-T_{b,r})-\hbar_{b2\mathrm{amb},r}A_{b2\mathrm{amb},r}(T_{b,r}-T_{\mathrm{amb}})] \tag{7b}$$

and the mixer

$$\frac{dT_{g,\mathrm{mx}}}{dt} = \frac{1}{m_{g,\mathrm{mx}}C_{g,\mathrm{mx}}}[W_{a,\mathrm{bp},i}C_{p,a}(T_{a,\mathrm{bp},o} - T_{g,\mathrm{mx},o}) + (W_{a,\mathrm{hm},i}C_{p,a} + W_{v,\mathrm{hm},o}C_{p,v})(T_{b,\mathrm{hm}} - T_{g,\mathrm{mx},o}) + \hbar_{b2g,\mathrm{mx}}A_{b2g,\mathrm{mx}}(T_{b,\mathrm{mx}} - T_{g,\mathrm{mx}})] \quad (8a)$$

$$\frac{dT_{b,\mathrm{mx}}}{dt} = \frac{1}{m_{b,\mathrm{mx}}C_{b,\mathrm{mx}}}[Q_{\mathrm{mx}} - \hbar_{b2g,\mathrm{mx}}A_{b2g,\mathrm{mx}}(T_{b,\mathrm{mx}} - T_{g,\mathrm{mx}}) - \hbar_{b2\mathrm{amb},\mathrm{mx}}A_{\mathrm{mx}}(T_{b,\mathrm{mx}} - T_{\mathrm{amb}})] \quad (8b)$$

Note again, the estimation of the water vapor mass flow rate, $W_{v,\mathrm{hm},o}$ in Eq. (8*b*), is presented in Eq. (1).

The lumped volume temperature state is considered either to be equal to the outlet temperature or the linear average between the inlet and outlet temperatures, depending upon the conditions of the control volume. After applying these relations, the measured control volume outlet conditions can be compared with the modeled estimates. These approximations are summarized by

$$T_{a,\mathrm{bp},o} = 2T_{\mathrm{bp}} - T_{a,\mathrm{bp},i}$$

$$T_{l,\mathrm{wh},o} = 2T_{l,\mathrm{wh}} - T_{l,r,o}$$

$$T_{l,\mathrm{hm},o} = 2T_{l,\mathrm{hm}} - T_{l,\mathrm{hm},i}$$

$$T_{l,r,o} = T_{l,r}$$

$$T_{g,\mathrm{hm},o} = 2T_{g,\mathrm{hm}} - T_{g,\mathrm{hm},i}$$

$$T_{g,\mathrm{mx}} = T_{g,\mathrm{mx},o} \quad (9)$$

Note, the reservoir and the mixer both receive two gas streams as inputs implying the assumption of a linear temperature distribution from the inlet to the outlet does not hold. Since both volumes are well mixed, it is instead assumed that the lumped temperature is equal to the outlet temperature.

4.3 Humidifier Model. The conservation of both mass and energy can be applied to a combination of the humidifier control volumes defined by the water, air/vapor mixture, and the bulk materials. It is important to re-emphasize here that this model is not intended for design purposes in which a detailed approximation of the spatial temperature distribution may be required. Rather an approximation of the control volume thermal response time is necessary for suitably tuning controllers capable of combining the moist and dry gas streams downstream of the humidifier. Here, we develop a simplified humidifier model to estimate the influence of the disturbances to the humidifier, such as the dry air mass flow rate, on the air and liquid water humidifier outlet temperatures.

In addition to the general assumptions made, A1–A4, we have employed the following additional assumptions specific to the humidifier:

- A5. The membrane thermal dynamics can be neglected. The thin polymeric membranes within the humidifier, of similar composition as the membranes employed in the fuel cell stack, are assumed to have no appreciable mass compared with the other control volumes, implying they do not store a significant amount of thermal energy.
- A6. The system can be adequately characterized by a two volume system comprised of the air volume (fast) and the liquid and bulk material volume (slow). Analysis on a three volume system, treating the air, liquid water, and bulk materials as separate volumes, indicated that there is little heat transfer between the bulk materials and the air, and a relatively large heat transfer between the liquid and the bulk materials, implying that the liquid and bulk can be treated as though they are in thermal equilibrium.
- A7. No liquid water transfers through the polymeric membrane.

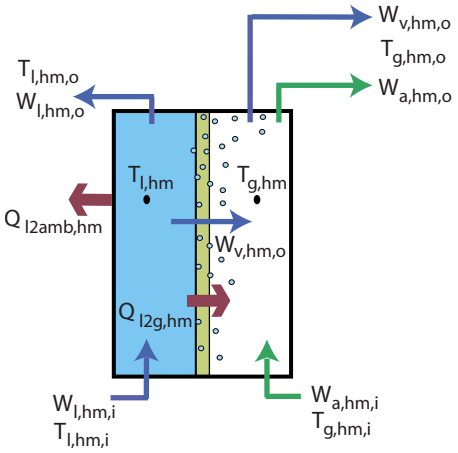

Fig. 9 Membrane based gas humidifier volumes

The inputs and outputs to the humidifier volumes are physically depicted in Fig. 9.

Applying the assumption of liquid and bulk thermal equilibrium results in a combination of the liquid water and bulk materials into a single control volume, which will be referred to as simply the humidifier water volume. The thermal dynamics of the water and gas can be modeled by applying the conservation of energy, such that

$$\frac{\partial U_{w,\mathrm{hm}}}{\partial dt} = W_{l,\mathrm{hm},i}h_{l,\mathrm{hm},i} - W_{l,\mathrm{hm},o}h_{l,\mathrm{hm},o} - W_{v,\mathrm{hm},o}h_{v,\mathrm{hm},o} - Q_{l2g,\mathrm{hm}} - Q_{l2\mathrm{amb},\mathrm{hm}} \quad (10a)$$

$$\frac{\partial U_{g,\mathrm{hm}}}{\partial dt} = W_{a,\mathrm{hm},i}h_{a,\mathrm{hm},i} - W_{a,\mathrm{hm},o}h_{a,\mathrm{hm},o} + Q_{l2g,\mathrm{hm}} \quad (10b)$$

where $\partial U_{w,\mathrm{hm}}/\partial dt$ and $\partial U_{g,\mathrm{hm}}/\partial dt$ represent the change in internal energy stored in the water and gas volumes, respectively; $Q_{l2g,\mathrm{hm}}$ is the heat transfer from the liquid water to the air through the membrane; $Q_{l2\mathrm{amb},\mathrm{hm}}$ is the heat transfer from the water volume to the ambient; $W_{l,\mathrm{hm},i}$ and $W_{l,\mathrm{hm},o}$ are the liquid water mass flow rates into and out of the humidifier; $W_{a,\mathrm{hm},i}$ and $W_{a,\mathrm{hm},o}$ are the dry air mass flow rates into and out of the humidifier; $W_{v,\mathrm{hm},o}$ is the water vapor mass flow exchanged through the membrane then leaving the humidifier entrained in the air exhaust stream; and h is the specific enthalpy of a constituent at the location indicated.

For simplicity, we have assumed that the water vapor enters and exits the humidifier air volume at the same temperature and therefore does not appear in the conservation of energy equation for the air volume. Additionally, in the experiments conducted in this work, the air supplied to the humidifier air volume was dry. Should moist air be supplied, an additional term must be added to the air volume of Eq. (10) to account for the specific enthalpy associated with any water vapor supplied with the air entering the air volume.

Applying the conservation of mass following assumption A2, the flow of liquid water entering the humidifier is equal to the sum of the liquid water and water vapor mass flow rates leaving the humidifier ($W_{l,\mathrm{hm},i} = W_{l,\mathrm{hm},o} + W_{v,\mathrm{hm},o}$) and the flow of dry air entering the humidifier is equal to that leaving the humidifier ($W_{a,\mathrm{hm},i} = W_{a,\mathrm{hm},o}$). Additionally, following assumption A3, all constituents have constant specific heat and behave ideally. Equation (10) can then be rewritten as

Table 2 Calibrated model parameters based on material properties

Mass (g)	Specific heat (J/kg K)	Area (m^2)
$m_{bp}=80$	$C_{bp}=460$	$A_{bp}=0.012$
$m_{l,wh}=50$	$C_{l,wh}=4180$	$A_{b2l,wh}=0.020$
$m_{b,wh}=780$	$C_{b,wh}=460$	$A_{wh}=0.028$
$m_{l,hm}=240$	$C_{l,hm}=4180$	$A_{l2amb,hm}=0.202$
$m_{a,hm}=18$	$C_{a,hm}=983$	$A_{l2g,hm}=0.03$
$m_{g,mx}=10$	$C_{g,mx}=863$	$A_{b2g,mx}=0.009$
$m_{b,mx}=745$	$C_{b,mx}=460$	$A_{mx}=0.012$
$m_{l,r}=2800$	$C_{l,r}=4180$	$A_{l2b,r}=0.075$
$m_{b,r}=1540$	$C_{b,r}=957$	$A_{b2amb,r}=0.087$
	$C_{p,a}=1004$	
	$C_{p,v}=1872$	
	$C_{p,l}=4180$	

$$\frac{dT_{l,\mathrm{hm}}}{dt}=\frac{1}{m_{l,\mathrm{hm}}C_{l,\mathrm{hm}}}[W_{l,\mathrm{hm},i}C_{p,l}(T_{l,\mathrm{hm},i}-T_{l,\mathrm{hm},o})-W_{v,\mathrm{hm},o}(h_{g,\mathrm{hm},o}-C_{p,l}T_{l,\mathrm{hm},o})-\hbar_{l2g,\mathrm{hm}}A_{l2g,\mathrm{hm}}(T_{l,\mathrm{hm}}-T_{g,\mathrm{hm}})-\hbar_{l2amb,\mathrm{hm}}A_{l2amb,\mathrm{hm}}(T_{l,\mathrm{hm}}-T_{\mathrm{amb}})] \tag{11a}$$

$$\frac{dT_{g,\mathrm{hm}}}{dt}=\frac{1}{m_{g,\mathrm{hm}}C_{g,\mathrm{hm}}}[W_{a,\mathrm{hm},i}C_{p,a}(T_{g,\mathrm{hm},i}-T_{g,\mathrm{hm},o})+\hbar_{l2g,\mathrm{hm}}A_{l2g,\mathrm{hm}}(T_{l,\mathrm{hm}}-T_{g,\mathrm{hm}})] \tag{11b}$$

where $h_{g,\mathrm{hm},o}$ is the specific enthalpy of water vapor at the temperature of the gas leaving the humidifier ($T_{g,\mathrm{hm},o}$). Consistent with the general two volume model presented, the humidifier volume inlet and outlet temperatures are assumed to be linear averages of their inlet and outlet conditions. Additionally, the water vapor mass flow leaving the humidifier $W_{v,\mathrm{hm},o}$ cannot be directly measured; therefore, an estimation is made as described in Eq. (1).

4.4 Calibrated Parameters, Inputs, and Outputs. The model parameters, specified by employing material properties and known dimensions, are listed in Table 2. For example, the mass of liquid water in the water heater was determined by measuring the internal volume and applying the average density of liquid water. The constant volume specific heats were calculated as mass weighted sums of the material components within the respective control volumes.

The locations of the measurements and disturbances were shown previously in Fig. 3. The inputs to the system are heater power (Q) and the mass fraction of air diverted through the bypass (r_{bp}); the states are the respective temperatures (T); the disturbances are the total dry air mass flow (W_a) and the air temperature supplied to the system ($T_{a,i}$); and the system output is the air relative humidity leaving the mixer ($\phi_{g,\mathrm{mx},o}$). It is important to note here that for controller simplicity, we have elected to hold the mass flow rate of liquid water circulated through the humidifier $W_{l,\mathrm{hm},i}$ constant. The need for control simplicity is not necessarily warranted for computational simplicity, but rather to avoid adding a pump motor controller (hardware and space cost) and an additional analog output to the data acquisition system. If it were desired to dynamically actuate the water circulating through the humidification system, this variable would be treated as a system input.

5 Parameter Identification

The heat transfer coefficients mostly affect the steady-state temperature of each volume, having little impact on the dynamic response. Hence, steady-state data can be employed at different air mass flow rates to numerically identify the heat transfer coefficients. However, numerous steady-state data would be required to identify the coefficients under a wide range of operating conditions. Additionally, physically realizing each steady-state condition requires a lengthy experiment considering some volumes have a relatively large thermal mass. Alternatively, dynamic experiments are completed to provide a rich data set for identification. The unknown parameters are tuned by minimizing the error between the measured and estimated outlet temperatures during both transient and quasi steady-state conditions.

Because the control volumes are cascaded, the control volume outlet temperature measurement is used for parameter identification of that control volume, and then can be used as a measured input for the subsequent control volume. To illustrate this more clearly, the mixer and bypass thermal dynamics from Eqs. (5) and (8) are rewritten to estimate the lumped control volume temperatures as

$$\frac{d\hat{T}_{a,\mathrm{bp}}}{dt}=\frac{1}{m_{\mathrm{bp}}C_{\mathrm{bp}}}[\bar{Q}_{\mathrm{bp}}+\bar{W}_{a,\mathrm{bp},i}C_{p,a}(\bar{T}_{a,\mathrm{bp},i}-\hat{T}_{a,\mathrm{bp},o})-\hbar_{b2amb,\mathrm{bp}}A_{b2amb,\mathrm{bp}}(\hat{T}_{a,\mathrm{bp}}-\bar{T}_{\mathrm{amb}})] \tag{12a}$$

$$\frac{d\hat{T}_{g,\mathrm{mx}}}{dt}=\frac{1}{m_{g,\mathrm{mx}}C_{g,\mathrm{mx}}}[\bar{W}_{a,\mathrm{bp},i}C_{p,a}(\bar{T}_{a,\mathrm{bp},o}-\hat{T}_{g,\mathrm{mx},o})+(\bar{W}_{a,\mathrm{hm},i}C_{p,a}+\bar{W}_{v,\mathrm{hm},o}C_{p,v})(\bar{T}_{g,\mathrm{hm},o}-\hat{T}_{g,\mathrm{mx},o})+\hbar_{b2g,\mathrm{mx}}A_{b2g,\mathrm{mx}}(\hat{T}_{b,\mathrm{mx}}-\hat{T}_{g,\mathrm{mx}})] \tag{12b}$$

$$\frac{d\hat{T}_{b,\mathrm{mx}}}{dt}=\frac{1}{m_{b,\mathrm{mx}}C_{b,\mathrm{mx}}}[\bar{Q}_{\mathrm{mx}}-\hbar_{b2g,\mathrm{mx}}A_{b2g,\mathrm{mx}}(\hat{T}_{b,\mathrm{mx}}-\hat{T}_{g,\mathrm{mx}})-\hbar_{b2amb,\mathrm{mx}}A_{b2amb,\mathrm{mx}}(\hat{T}_{b,\mathrm{mx}}-\bar{T}_{\mathrm{amb}})] \tag{12c}$$

where an overbar ($\bar{x}$) is used to denote measured values, and a hat ($\hat{x}$) is used for estimated quantities. For example, the mixer utilizes measured temperatures of the air supplied from the bypass, rather than model estimates. However, in tuning the bypass model, the bypass air outlet temperature is an estimate that can be compared with the measured value for parameter tuning.

The reservoir, water heater, and humidifier, make up a closed water circulation system. As a result, if the estimation of temperature anywhere in this loop is inaccurate, the error will propagate through the subsequent control volumes. For control purposes, a measurement of the water temperature in this circulation system is not necessary. As a result, it is imperative that the models of these three control volumes approximate the response to inputs and disturbances very well, otherwise a measurement of temperature somewhere in this loop would be required for compensation. To ensure that estimation errors do not propagate, first, the water circulation system was tuned by identifying the parameters associated with the humidifier and water heater independent of the other control volumes. Then, the parameters associated with the reservoir control volume were determined by including the identified humidifier and water heater model estimates. This process is detailed by indicating the measurements and estimates in the following state equations

$$\frac{d\hat{T}_{l,\mathrm{wh}}}{dt}=\frac{1}{m_{l,\mathrm{wh}}C_{l,\mathrm{wh}}}[\bar{W}_{l,\mathrm{hm},i}C_{p,l}(\bar{T}_{l,r,o}-\hat{T}_{l,\mathrm{hm},i})+\hbar_{b2l,\mathrm{wh}}A_{b2l,\mathrm{wh}}(\hat{T}_{b,\mathrm{wh}}-\hat{T}_{l,\mathrm{wh}})] \tag{13a}$$

$$\frac{d\hat{T}_{b,\mathrm{wh}}}{dt}=\frac{1}{m_{b,\mathrm{wh}}C_{b,\mathrm{wh}}}[\bar{Q}_{\mathrm{wh}}-\hbar_{b2l,\mathrm{wh}}A_{b2l,\mathrm{wh}}(\hat{T}_{b,\mathrm{wh}}-\hat{T}_{l,\mathrm{wh}})-\hbar_{b2amb,\mathrm{wh}}A_{b2amb,\mathrm{wh}}(\hat{T}_{b,\mathrm{wh}}-\bar{T}_{\mathrm{amb}})] \tag{13b}$$

$$\frac{d\hat{T}_{l,\mathrm{hm}}}{dt} = \frac{1}{m_{l,\mathrm{hm}}C_{l,\mathrm{hm}}}[\bar{W}_{l,\mathrm{hm},i}C_{p,l}(\bar{T}_{l,\mathrm{hm},i} - \hat{T}_{l,\mathrm{hm},o}) - \hat{W}_{v,\mathrm{hm},o}(\hat{h}_{g,\mathrm{hm},o} - C_{p,l}\hat{T}_{l,\mathrm{hm},o}) - \hbar_{l2g,\mathrm{hm}}A_{l2g,\mathrm{hm}}(\hat{T}_{l,\mathrm{hm}} - \hat{T}_{g,\mathrm{hm}}) - \hbar_{l2\mathrm{amb,hm}}A_{l2\mathrm{amb,hm}}(\hat{T}_{l,\mathrm{hm}} - \bar{T}_{\mathrm{amb}})] \quad (13c)$$

$$\frac{d\hat{T}_{g,\mathrm{hm}}}{dt} = \frac{1}{m_{g,\mathrm{hm}}C_{g,\mathrm{hm}}}[\bar{W}_{a,\mathrm{hm},i}C_{p,a}(\bar{T}_{g,\mathrm{hm},i} - \hat{T}_{g,\mathrm{hm},o}) + \hbar_{l2g,\mathrm{hm}}A_{l2g,\mathrm{hm}}(\hat{T}_{l,\mathrm{hm}} - \hat{T}_{g,\mathrm{hm}})] \quad (13d)$$

$$\frac{d\hat{T}_{l,r}}{dt} = \frac{1}{m_{l,r}C_{l,r}}[\bar{W}_{l,\mathrm{fc},i}C_{p,l}(\bar{T}_{l,\mathrm{fc},o} - \hat{T}_{l,r,o}) + \bar{W}_{l,\mathrm{wh},i}C_{p,l}(\hat{T}_{l,\mathrm{hm},o} - \hat{T}_{l,r,o}) - \hbar_{l2b,r}A_{l2b,r}(\hat{T}_{l,r} - \hat{T}_{b,r})] \quad (13e)$$

$$\frac{d\hat{T}_{b,r}}{dt} = \frac{1}{m_{b,r}C_{b,r}}[\hbar_{l2b,r}A_{l2b,r}(\hat{T}_{l,r} - \hat{T}_{b,r}) - \hbar_{b2\mathrm{amb},r}A_r(\hat{T}_{b,r} - \bar{T}_{\mathrm{amb}})] \quad (13f)$$

For the bypass, mixer, water heater, and reservoir, the cost function $J=\frac{1}{n}\Sigma_{i=1}^{n}(\bar{T}-\hat{T})^2$, where n is the number of data points in the experiment, is minimized by adjusting the unknown parameter values using unconstrained nonlinear minimization. Note, the unknown heat transfer coefficients are either constant or a function of the gas or liquid mass flow rates. If all parameters were constant, a linear least-squares estimation could be employed.

In tuning the humidifier as a combined two volume system, the cost function

$$J = \frac{1}{n}\sum_{i=1}^{n}(\bar{T}_{g,\mathrm{hm},o} - \hat{T}_{g,\mathrm{hm},o})^2 + (\bar{T}_{l,\mathrm{hm},o} - \hat{T}_{l,\mathrm{hm},o})^2 \quad (14)$$

was employed, modified from the single volume cost functions described above, to simultaneously penalize the error of both the air and the water temperature estimations. Weights could be used to place more importance on the air or water temperature estimations, if desired. Note, although the mixer, water heater, and reservoir control volumes are also two volume systems, measurements of the bulk stainless steel temperatures are not available. As a result, these volumes are tuned using only the air/liquid water temperature estimation errors.

Experiments were conducted to identify the unknown heat transfer coefficients in the humidification system model. These experiments included multiple steps in the resistive heater power, along with steps in the total dry air mass flow supplied to the humidification system to mimic the air mass flow demand due to changes in the PEMFC electrical load. Throughout these experiments, the fuel cell system is not connected to the humidification system. Instead, a manual valve was placed downstream of the mixer to simulate the effect of the fuel cell back pressure. Care was taken to minimize the time at which the bypass outlet temperature was colder than the humidifier outlet temperature to minimize the formation of condensate. Additionally, the mixer outlet was kept at a higher temperature than the humidifier and bypass outlets for this same reason.

As described previously, these temperature estimations relied on the assumption that the humidifier air outlet is fully saturated $\phi_{g,\mathrm{hm},o}=1$ in order to calculate the water vapor mass flow rate. For other membrane based systems in which the humidifier air outlet is not fully saturated, a measurement of this relative humidity must be made.

Table 3 Tuned humidification system model parameters based on experimental identification

Expected range[a]	Identified value ($\mathrm{W/m^2\,K}$)
50–20,000	$\hbar_{b2l,\mathrm{wh}}=139.8$ and $\hbar_{l2b,r}=167.5$
50–1000	$\hbar_{b2\mathrm{amb,wh}}=0$ and $\hbar_{l2\mathrm{amb,hm}}=14.6$
	$\hbar_{b2\mathrm{amb},r}=80.0$
5–250	$\hbar_{\mathrm{bp}}=10.8-21{,}822W_{a,\mathrm{bp},i}$
5–25	$\hbar_{b2\mathrm{amb,mx}}=25.8$
25–250	$\hbar_{b2g,\mathrm{mx}}=2819W_{a}^{0.54}$
25–20,000	$\hbar_{l2g,\mathrm{hm}}=41{,}244W_{a,\mathrm{hm},i}^{0.95}$

[a]Expected ranges taken from Ref. [16] for natural and forced convections of liquids and gases.

The identified heat transfer coefficients are summarized in Table 3. As described in Sec. 4, these coefficients can take on different functional forms depending upon the heat transfer process taking place. For all control volumes, constant heat transfer coefficients were considered for the heat transfer between the bulk materials and the gas or liquid water to reduce the number of identified parameters. Interestingly, for heat transfer occurring between bulk materials and liquid water, a constant heat transfer coefficient accurately captured the steady-state temperature and was therefore used due to simplicity rather than employing the variable heat transfer coefficient. Finally, due to the simplification of the bypass control volume from a two state to a single state system, the heat transfer loss from the control volume was assumed to be a linear function of flow rate of the form $\hbar_{\mathrm{bp}}=\beta_{1,\mathrm{bp}}+\beta_{2,\mathrm{bp}}W_{a,\mathrm{bp},i}$. All of the identified parameters are close or within the expected parameter ranges.

6 Model Validation

For validating the model, all of the control volumes were combined such that the estimation of the temperature leaving one control volume is treated as an input to subsequent control volumes, as shown in Fig. 10. An experiment, different than that used for parameter identification, was conducted for validating the model. This experiment included steps in the air mass flow rate as well as the heaters.

The estimated bypass air outlet temperature is compared with the measurement in Fig. 11. For changes in the air mass flow rate and the bypass heater, the model captures the response time. However, there is an offset in the steady-state temperature estimation throughout most of the experiment, due to an overestimation of the heat loss from the control volume to the ambient. Linearization of the bypass state equation has shown that the bypass pole

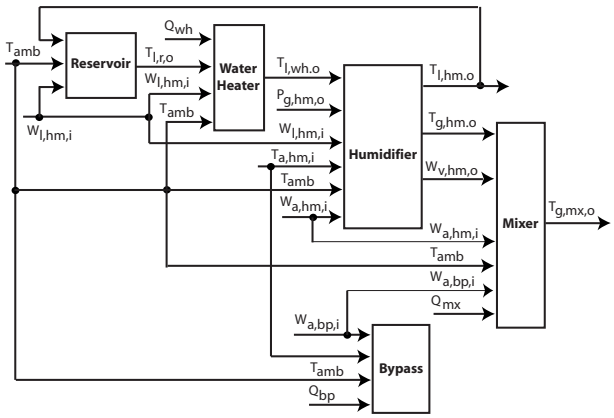

Fig. 10 Model structure for open the loop simulation of the gas humidification system

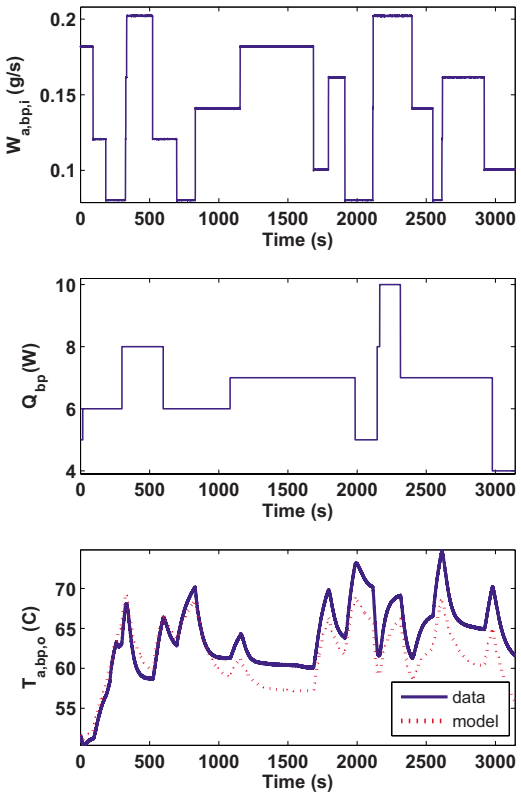

Fig. 11 Bypass experimental validation results. Given the measured air mass flow rate and temperature of the air supplied to the bypass, the air outlet temperature is estimated and compared with measurements.

location is most sensitive to air flow and not the heat transfer coefficient. As a result, this steady-state error will have little impact on the resulting controller design. Additionally, this estimation offset has little impact on the gas mixer temperature estimation due to the relatively small fraction of air flowing through the bypass as compared with the humidifier. However, care should be taken in applying this bypass model beyond its intended use for the controller design. The average estimation error was 2.8°C with a standard deviation of 1.4°C.

The estimated water reservoir outlet temperature is compared with the measurement in Fig. 12. The reservoir system is driven by the estimate of the liquid water temperature leaving the humidifier and represents a significant thermal lag in the water circulation system due to the relatively large stored water mass. The reservoir model captures both the slow response following the humidifier dynamics as well as the steady-state temperature. The average estimation error was 0.3°C with a standard deviation of 0.2°C.

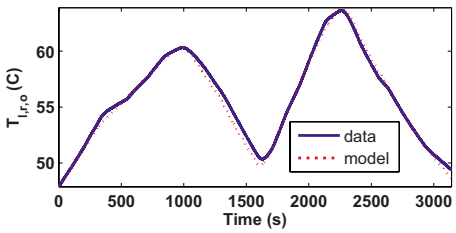

Fig. 12 Reservoir validation results. Given the measured liquid water mass flow rate and the estimated liquid water temperature supplied to the reservoir, the liquid water outlet temperature is estimated.

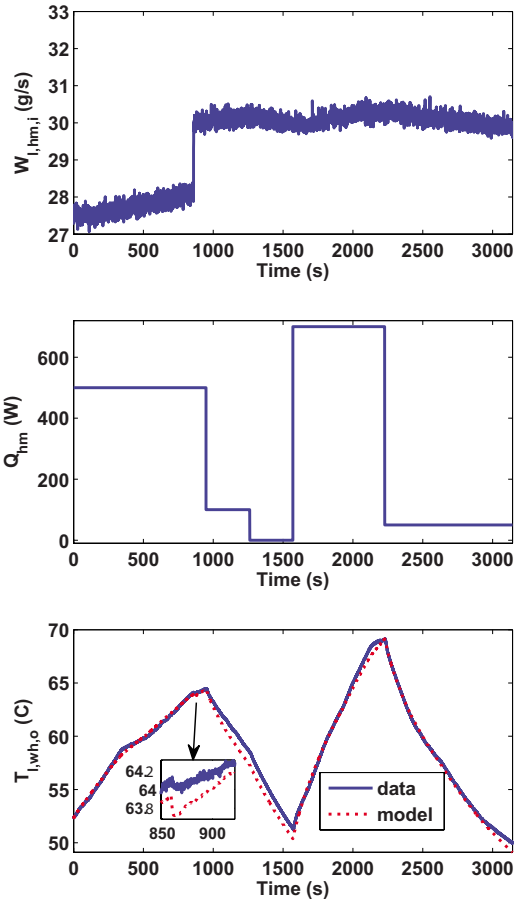

Fig. 13 Water heater validation results. Given the measured liquid water mass flow rate supplied and the estimated inlet temperature, the liquid water outlet temperature is estimated.

The estimated water heater outlet temperature is compared with the measurement in Fig. 13. The water heater model captures the slow response due to changes in the heater as well as the steady-state temperature. Note, at approximately 860 s, the liquid water mass flow rate through the water heater was increased by changing the manual throttle valve position. This flow increase caused a decrease in the water heater temperature, which was well approximated by the model. Although we have framed the control problem here such that the liquid water mass flow rate is not actuated, we elected to add this disturbance during model validation to ensure that the model accurately captures the system response to liquid water flow changes to enable future controller development. The average estimation error was 0.4°C with a standard deviation of 0.3°C.

The estimated air and liquid water temperatures leaving the humidifier are compared with the measurements in Fig. 14. The humidifier air outlet temperature estimation has a steady-state offset when the system is cooling down (from approximately 1000–1500 s to 2300–3000 s). This offset is thought to be the result of neglecting the condensation or evaporation of water on the air side of the humidifier, a complex process that has been neglected here. However, the air temperature is well approximated during warm-up and captures the correct dynamic response throughout the experiment. The response of the liquid water is well approximated throughout the experiment. Considering the complexity of the physical humidifier system, and the modeling assumptions made, this model adequately captures the humidifier thermal response. The average estimation errors were 1.2°C and 0.6°C with standard deviations of 1.1°C and 0.5°C, for the air and liquid water, respectively.

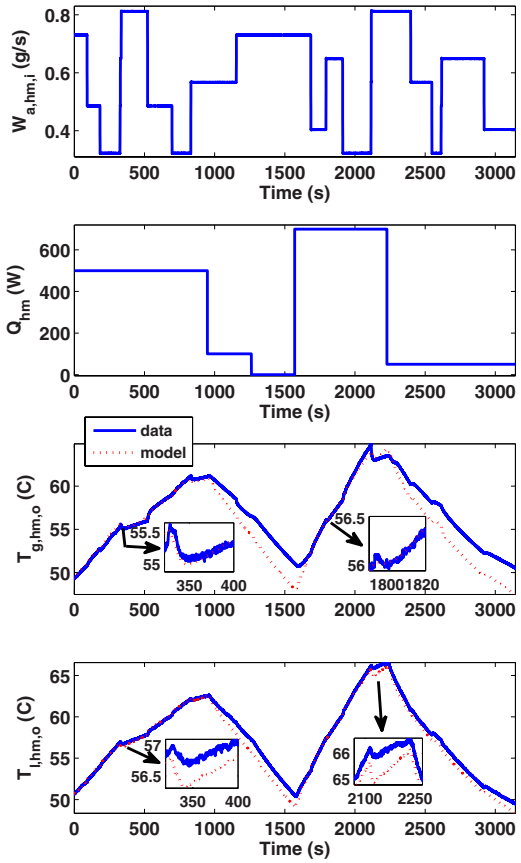

Fig. 14 Humidifier validation results. Given the measured air and liquid water mass flow rates supplied, the estimated liquid water inlet temperature, and the measured air inlet temperature, the air and liquid water outlet temperatures are estimated.

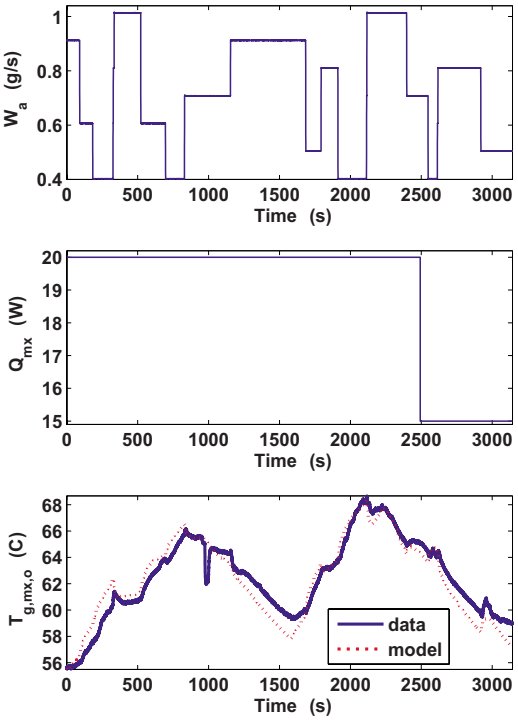

Fig. 15 Mixer validation results. Given the measured air mass flow rate and estimated bypass and humidifier air outlet temperatures supplied to the mixer, the mixer air outlet temperature is estimated.

The estimated mixer air outlet temperature is compared with the measurement in Fig. 15. The mixer response to changes in air mass flow rate or mixer heat is well captured throughout the experiment. An improvement in the humidifier estimation during the cool down portion of the experiment may improve the mixer estimation during this period. Note, at approximately 1000 s, the measured mixer outlet temperature momentarily decreases dramatically. The cause of this rapid decrease and then increase in temperature is unknown but was an isolated event that could not be reproduced. The average estimation error was 0.9°C with a standard deviation of 0.6°C.

7 Control and System Design

Although the humidification system model presented in this work was derived for the purpose of developing control methodologies for active humidity and thermal management, it can be applied to evaluate component sizing under steady conditions. It is important, however, to remember that the gas humidification system model is intended for dynamic regulation. It is not the static power consumption that is of concern for controller development, rather the total energy required to transition from one set of operating conditions to another. This energy consumption is dependent upon the control architecture selected, as well as actuator and sensor placements, which is discussed in the second part of this two-paper series.

There are several system design variables that will influence the overall energy efficiency at a given set of operating conditions. Two critical variables are the heat loss from the control volumes and the fuel cell coolant outlet temperature supplied to the water reservoir. Any heat lost to the ambient, must be supplied by the heaters somewhere in the system. Thus, it seems logical to minimize heat loss from the various control volumes. However, by minimizing heat loss, the system transient response is sacrificed when transitioning from one setpoint temperature to a lower setpoint temperature, during which heat must be quickly rejected from the system. Thus, a balance must be struck between system energy efficiency under steady conditions and the ability of the system to quickly regulate temperature and humidity in response to system disturbances.

The fuel cell stack is an important element of the gas humidification system in that it provides an energy input into the water reservoir (via the fuel cell coolant exhaust stream) and is often used to specify the temperature at which the reactants are supplied to the fuel cell stack $T^*_{g,\mathrm{mx},o}$. This energy input to the water reservoir is appreciable and reduces the thermal load on the heat exchangers within the fuel cell water coolant circulation system. If an internal gas humidifier were to be compared with this humidification methodology, waste heat from the fuel cell stack would be considered as an energy input through material conduction from the power section to the humidification section of the fuel cell stack.

Without considering the fuel cell coolant energy injection, the amount of energy required to provide humidified air to the fuel cell is approximately equal to the energy of evaporation, as shown in Fig. 16 as a function of the desired mixer outlet (cathode inlet) temperature $T_{g,\mathrm{mx},o}$. The fuel cell stack that this work has been based on has a typical operating temperature of approximately 65°C. From a sizing perspective, the water heater must be adequately sized to overcome the energy required for evaporation as well as the comparatively small heat losses from the control volumes. Additionally, this energy demand increases with increased air mass flow (load demand). Should this system be run at 0.45 A/cm^2, with an air stoichiometry of 250%, and a desired cathode inlet temperature of 80°C and fully humidified, the water heater could just meet this demand. In this manner, this model could be used to compare the tradeoffs associated with control

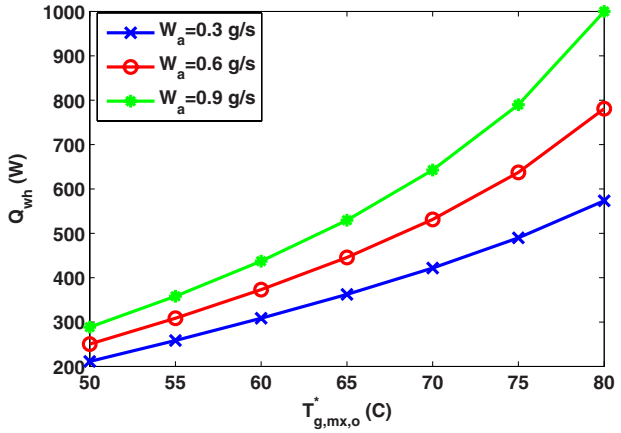

Fig. 16 Required water heater input Q_{wh} necessary as a function of total dry air mass flow rate W_a and desired cathode inlet temperature $T_{g,mx,o}$ under steady conditions. The air mass flow rates selected correspond to changes in the current density from the nominal operating conditions (W_a=0.6 g/s) to 0.15 A/cm^2 (W_a=0.3 g/s) and 0.45 A/cm^2 (W_a=0.9 g/s).

architecture and system design. For example, providing energy to the humidification system via the fuel cell coolant loop, at the cost of decreased relative humidity, as opposed to resizing components.

8 Conclusions

An apparatus was devised to regulate the temperature and relative humidity of reactant gases supplied to a fuel cell. For controller development, a physics based, control-oriented model of the thermal and humidity dynamics of this membrane-type humidification system was developed and experimentally validated. The humidity dynamics are accurately estimated under a range of operating conditions using a simple nonlinear output equation. The thermal dynamics of the various control volumes, related time constants, and impact of the operating conditions on the thermal response are modeled to generate an accurate approximation of system temperatures. With this model of a humidification system, controllers can be designed and implemented to regulate the exhaust relative humidity and temperature despite disturbances in the air mass flow rate. Incidentally, this model could be used under steady conditions for component sizing. Part B of this work will employ this humidification system model to design and implement controllers that regulate the exhaust relative humidity and temperature despite disturbances in air mass flow rate.

Acknowledgment

We gratefully acknowledge funding from the U.S. Army Center of Excellence for Automotive Research (Grant No. DAAE07-98-3-0022) and the National Science Foundation (Grant No. CMS 0625610).

Nomenclature

Variables

A = surface area available for heat transfer (m^2)
C_p = constant pressure specific heat (J/kg K)
C = constant volume specific heat (J/kg K)
$\hbar$ = heat transfer coefficient (W/m^2 K)
h = specific enthalpy (J/kg)
m = mass (kg)
M = molecular weight (kg/mol)
p = pressure (Pa) or pole location
r = mass flow ratio
t = time (s)
T = temperature (K)
W = mass flow rate (kg/s)
β = heat transfer coefficient parameters
ϕ = relative humidity (0–1)
ω = humidity ratio

Subscript and Superscript Symbols

a = air
amb = ambient
bp = bypass
b = control volume bulk materials
cv = control volume
fc = fuel cell stack
g = gas constituent
hm = humidifier
i = into the control volume
l = liquid water
mx = mixer
o, out = out of the control volume
r = reservoir
sat = saturation
v = water vapor
wc = water circulation system (humidifier, reservoir, and water heater)
wh = water heater

References

[1] Muller, E., Stefanopoulou, A., and Guzzella, L., 2007, "Optimal Power Control of Hybrid Fuel Cell Systems for an Accelerated System Warm-Up," IEEE Trans. Control Syst. Technol., **15**(2), pp. 290–305.
[2] McKay, D., Siegel, J., Ott, W., and Stefanopoulou, A., 2008, "Parameterization and Prediction of Temporal Fuel Cell Voltage Behavior During Flooding and Drying Conditions," J. Power Sources, **178**(1), pp. 207–222.
[3] Karnik, A., Stefanopoulou, A., and Sun, J., 2007, "Water Equilibria and Management Using a Two-Volume Model of a Polymer Electrolyte Fuel Cell," J. Power Sources, **164**, pp. 590–605.
[4] Rajalakshmi, N., Sridhar, P., and Dhathathreyan, K., 2002, "Identification and Characterization of Parameters for External Humidification Used in Polymer Electrolyte Membrane Fuel Cells," J. Power Sources, **109**(2), pp. 452–457.
[5] Love, A., Middleman, S., and Hochberg, A., 1993, "The Dynamics of Bubblers as Vapor Delivery Systems," J. Cryst. Growth, **129**, pp. 119–133.
[6] Reid, R., 2002, "Humidification of a PEM Fuel Cell by Air-Air Moisture," U.S. Patent No. 6,403,249.
[7] Shimanuki, H., Katagiri, T., Suzuki, M., and Kusano, Y., 2002, "Humidifier for Use With a Fuel Cell," U.S. Patent No. 6,471,195.
[8] Choi, K., Park, D., Rho, Y., Kho, Y., and Lee, T., 1998, "A Study of the Internal Humidification of an Integrated PEMFC Stack," J. Power Sources, **74**, pp. 146–150.
[9] Staschewski, D., 1996, "Internal Humidifying of PEM Fuel Cells," Int. J. Hydrogen Energy, **21**(5), pp. 381–385.
[10] Mueller, E., and Stefanopoulou, A., 2005, "Analysis, Modeling, and Validation for the Thermal Dynamics of a Polymer Electrolyte Membrane Fuel Cell Systems," ASME Paper No. FUELCELL2005-74050.
[11] Chen, D., and Peng, H., 2005, "A Thermodynamic Model of Membrane Humidifiers for PEM Fuel Cell Humidification Control," Trans. ASME, J. Dyn. Syst. Meas., **127**, pp. 424–432.
[12] Wheat, W., Clingerman, B., and Hortop, M., 2005, "Electronic By-Pass Control of Gas Around the Humidifier to the Fuel Cell," U.S. Patent No. 6,884,534.
[13] Vermillion, C., Sun, J., Butts, K., and Hall, A., 2006, "Modeling and Analysis of a Thermal Management System for Engine Calibration," *Proceedings of the 2006 IEEE International Conference*.
[14] Cortona, E., Onder, C., and Guzzella, L., 2002, "Engine Thermomanagement With Electrical Components for Fuel Consumption Reduction," Int. J. Engine Res., **3**(3), pp. 157–170.
[15] Setlur, P., Wagner, J., Dawson, D., and Marotta, E., 2005, "An Advanced Engine Thermal Management System: Nonlinear Control and Test," IEEE/ASME Trans. Mechatron., **10**(2), pp. 210–220.
[16] Sonntag, R. E., Borgnakke, C., and Van Wylen, G. J., 2003, *Fundamentals of Thermodynamics*, Wiley, New York.